THE AMERICAN SOCIETY OF MECHANICAL ENGINEERS
345 E. 47 St., New York, N.Y. 10017

92-GT-126

117

The Effect of Inlet Swirl on the Rotordynamic Shroud Forces in a Centrifugal Pump

A. GUINZBURG, C. E. BRENNEN, A. J. ACOSTA and T. K. CAUGHEY
California Institute of Technology
Division of Engineering and Applied Science
Pasadena, California 91125

ABSTRACT

The role played by fluid forces in determining the rotordynamic stability of a centrifugal pump is gaining increasing attention. The present research investigates the contributions to the rotordynamic forces from the discharge-to-suction leakage flows between the front shroud of the rotating impeller and the stationary pump casing. In particular, the dependency of the rotordynamic characteristics of leakage flows on the swirl at the inlet to the leakage path was examined. An inlet guide vane was designed for the experiment so that swirl could be introduced at the leakage flow inlet. The data demonstrates substantial rotordynamic effects and a destabilizing tangential force for small positive whirl ratios; this force decreased with increasing flow rate. The effect of swirl on the rotordynamic forces was found to be destabilizing.

NOMENCLATURE

$[A^*]$	rotordynamic matrix
$[A]$	rotordynamic matrix, normalized by $\rho\pi\omega^2 R_2{}^3 L$
B	depth of inlet guide vane
C,c	rotordynamic damping coefficients, normalized by $\rho\pi\omega R_2{}^3 L$
$F^*(t)$	hydrodynamic forces
$F(t)$	hydrodynamic forces, normalized by $\rho\pi\omega^2 R_2{}^3 L\varepsilon/R_2$
$F^*_x(t),F^*_y(t)$	Lateral forces on the rotating shroud in the stationary laboratory frame
$F_x(t),F_y(t)$	Lateral forces on the rotating shroud in the stationary laboratory frame, normalized by $\rho\pi\omega^2 R_2{}^3 L\varepsilon/R_2$
F^*_{ox},F^*_{oy}	steady hydrodynamic forces
F_{ox},F_{oy}	steady hydrodynamic forces, normalized by $\rho\pi\omega^2 R_2{}^3 L$
$F^*_n(t),F^*_t(t)$	unsteady hydrodynamic forces
$F_n(t),F_t(t)$	unsteady hydrodynamic forces, normalized by $\rho\pi\omega^2 R_2{}^3 L\varepsilon/R_2$
H	shroud clearance between rotor and casing
K,k	rotordynamic stiffness coefficients, normalized by $\rho\pi\omega^2 R_2{}^3 L$
L	axial length of the shroud
M,m	rotordynamic inertial coefficients, normalized by $\rho\pi R_2{}^3 L$
Q	volume flow rate
R	shroud radius
Re_φ	Axial flow Reynolds number based on axial flow, $2HU_s/\nu$
Re_ω	Rotaional Reynolds number based on tip speed, $\omega R_2{}^2/\nu$
t	time
u_s	mean inlet swirl velocity of the fluid
u_θ	mean inlet swirl velocity of the fluid
$x^*(t)$	instantaneous displacement in the x direction, normalized by the leakage inlet radius, R_2.

Presented at the International Gas Turbine and Aeroengine Congress and Exposition
Cologne, Germany June 1-4, 1992
This paper has been accepted for publication in the Transactions of the ASME
Discussion of it will be accepted at ASME Headquarters until September 30, 1992

$y^*(t)$	instantaneous displacement in the y direction, normalized by the leakage inlet radius, R_2.
α	turning angle of the flow
Γ	swirl ratio of fluid tangential velocity to rotor tip velocity, $u_\theta/\omega R_2$
δ	offset or distance between the center of the whirl orbit and the center of the stationary casing.
ε	eccentricity or radius of the whirl motion.
ν	dynamic viscosity of the fluid
ρ	density of the fluid
ϕ	flow coefficient, $Q/2\pi R_2^2 H\omega$
ω	rotor frequency
Ω	whirl frequency

1. INTRODUCTION

In turbomachinery, the trend toward higher speeds and higher power densities has led to an increase in the number and variety of fluid-structure interaction problems in pumps, compressors, turbines and other machines. This occurs because the typical fluid forces scale like the square of the speed and thus become increasingly important relative to the structural strength. This becomes particularly acute in rocket engine turbopumps where demands to minimize the turbopump mass may also lead to reductions in the structural strength. Consequently designers and manufacturers are concerned with the fluid induced rotordynamic forces on impellers in turbomachines. Knowledge of the steady and unsteady forces and the associated rotordynamic coefficients is required to effectively model the rotordynamics of high speed turbomachines.

2. BACKGROUND

Rotordynamic forces imposed on a centrifugal pump by the fluid flow through it were first measured by Domm and Hergt (1970), Hergt and Krieger (1969-70), Chamieh et al. (1985) and Jery et al. (1985). In the Rotor Force Test Facility (RFTF) at Caltech (Jery et al., 1985; Adkins et al., 1988; Franz et al., 1989) known whirl motions over a full range of frequencies (subsynchronous, supersynchronous as well as reverse whirl) are superimposed on the normal motion of an impeller.

The hydrodynamic force on a rotating shroud or impeller (see figure 1) which is whirling can be expressed in the stationary laboratory frame in linear form as:

$$\begin{bmatrix} F^*_x(t) \\ F^*_y(t) \end{bmatrix} = \begin{bmatrix} F^*_{ox} \\ F^*_{oy} \end{bmatrix} + [A^*] \begin{bmatrix} x^*(t) \\ y^*(t) \end{bmatrix} \qquad (1)$$

The first term on the right hand side represents the radial force in the absence of whirl motion, so that F^*_{ox}, F^*_{oy} are the steady, time-averaged forces in a stationary frame which result from flow asymmetries in the volute or the

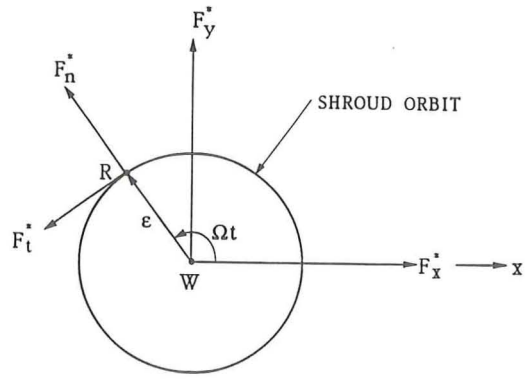

Figure 1. Schematic of the fluid-induced radial forces acting on an impeller whirling in a circular orbit. F^*_x and F^*_y represent the instantaneous forces in the stationary laboratory frame. F^*_n and F^*_t are the forces normal and tangential to the whirl orbit where Ω is the whirl frequency.

inlet duct. These steady radial forces are discussed in detail elsewhere (Iverson et al. [1960], Domm and Hergt [1970], Chamieh [1983], Chamieh et al. [1985], Adkins [1986]). The matrix $[A^*]$ is the rotordynamic matrix which operates on the instantaneous displacement $[x^*]$ of the rotor center. Note that $[A^*]$ will in general be a function not only of the mean flow conditions and pump geometry but also of the frequency of whirl, Ω. If outside the linear range, it may also be a function of the amplitude of the whirl motion, ε. At small, linear amplitudes $[A^*]$ should be independent of ε and presented as a function of the whirl ratio Ω/ω where ω is the impeller rotation frequency. In the case of a circular whirl orbit $x^* = \varepsilon\cos\Omega t$, $y^* = \varepsilon\sin\Omega t$. Then the forces normal and tangential to the imposed circular whirl orbit are related to the matrix elements as follows:

$$F_n^*(t) = \frac{1}{2}(A^*_{xx} + A^*_{yy})\varepsilon$$

$$F_t^*(t) = \frac{1}{2}(-A^*_{xy} + A^*_{yx})\varepsilon \qquad (2)$$

The reader is referred to Jery et al (1985) and Franz et al. (1989) for details. In the analysis which follow, the above equations will be expressed in non dimensional terms. If in addition, [A] is to be rotationally invariant, then

$$A_{xx} = A_{yy} = F_n$$

$$A_{xy} = -A_{yx} = F_t \qquad (3)$$

When it became apparent that leakage flows could contribute significantly to the rotordynamics of a pump, Childs (1989) adapted the bulk-flow model which was developed for the analysis of fluid-induced forces in seals to evaluate the rotordynamic forces, F_n and F_t, due to these leakage flows. The magnitude and overall form of the model predictions are consistent with the experimental data. In the context of the present paper, Childs' theory yielded some unusual results, including peaks in the rotordynamic forces at particular positive whirl ratios. This phenomenon was tentatively described as a "resonance" of the leakage flow. Childs suggested that this unexpected phenomenon develops at small positive whirl

ratios when the inlet swirl velocity ratio exceeds about 0.5. It remains to be seen whether such "resonances" occur in practice. Childs (1986) points out that a typical swirl velocity ratio at inlet (pump discharge) would be about 0.5 and may not therefore be large enough for the resonance to be manifest. There have been reports that SSME impellers fitted with anti-swirl vanes in the leakage flow annulus have had noticeably different rotordynamic characteristics (Childs et al. [1990a,b]). These results were partly responsible for motivating the present investigations of the dependency of the normal and tangential forces on the swirl at the inlet to the leakage path.

3. LEAKAGE FLOW TEST APPARATUS

A detailed description of the test facility, can be found in many of the references (Chamieh[1983], Adkins[1986], Jery[1986], Arndt[1988], Franz[1989]), so only a brief description will be given here. The experiments were conducted in the Rotor Force Test Facility(RFTF), which was constructed to study fluid induced forces on an impeller whirling around the machine axis of rotation. The experimental objective was to impose well controlled rotations and whirl motions on a very stiff impeller/shaft system and to measure directly the resulting force on the impeller. This is accomplished by the eccentric drive mechanism which superposes a circular orbit on the basic rotation. The shroud is mounted on a spindle attached to the rotating force balance (Jery et al. [1985], Franz et al. [1989]), which measures the forces directly on the shroud. The rotating dynamometer permits measurements of the rotordynamic force matrix due to the shroud fluid forces. The experimental apparatus sketched in figures 2 was designed and constructed to simulate the leakage flow along the shroud from the impeller discharge to the impeller inlet (Zhuang [1989], Guinzburg et al. [1990], Guinzburg et al. [1992]). The clearance between the rotating shroud and the stationary casing can be varied by both axial and radial adjustment of the stationary casing. For the present experiment, the initial geometric configuration consists of a straight annular gap inclined at an angle of 45° to the axis of rotation. The schematic in figure 3 shows the clearance in the centered position when the centers of the shroud and the casing both coincide. In order to model losses in the flow, an adjustable seal ring was used (refer to figure 2). The face seal clearance in this experiment permits the pressure drop to be separately adjusted from the flow.

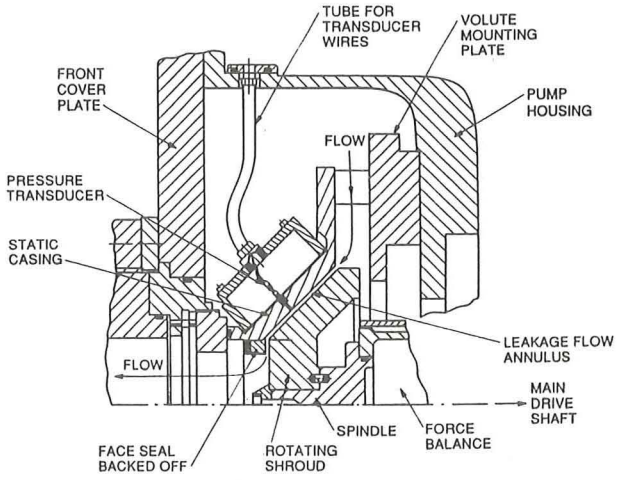

Figure 2 Layout of the leakage flow test apparatus for installation in the RFTF. (Zhuang [1989]).

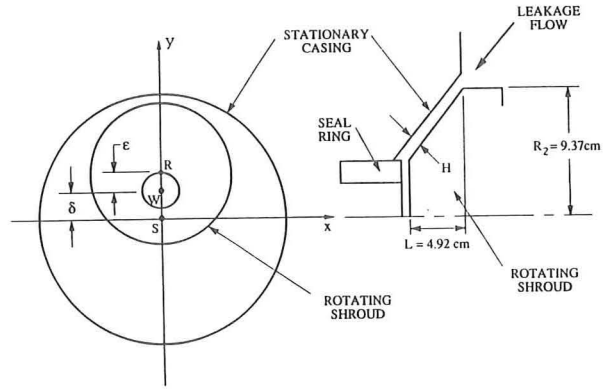

Figure 3 Schematic of the whirling shroud where S is the center of the stationary casing, R is the center of the rotating shroud, W is the center of the whirl orbit along which R travels, WR = ε is the eccentricity, and WS = δ is the offset.

The flow through the leakage path is generated by an auxiliary pump and the selection of the flow rates through the leakage path was based on performance characteristics of a typical centrifugal pump. The shroud can be driven at speeds up to 3500 RPM and a circular whirl motion with a frequency up to 1800 RPM can be superimposed on the basic rotation. The eccentric drive mechanism permits testing with the amplitude of the whirl motion or eccentricity, ε adjustable from 0.000 cm. to 0.152 cm. Further details on the experimental equipment can be found in Guinzburg (1992). The results from these experiments will be presented non-dimensionally by dividing the forces by $\rho\pi\omega^2 R_2^3 L\varepsilon/R_2$.

As was mentioned previously, the inlet tangential velocity to the leakage path was shown by Childs(1989) to have an effect on the rotordynamic forces. Consequently, the effect of swirl was investigated by installing a device that was used to introduce pre rotated fluid, in the direction of shaft rotation, at the shroud inlet. This was accomplished by constraining the flow in a logarithmic spiral channel. The inlet swirl vane was designed with sufficient solidity to create an isotropic inlet flow. The turning angle was chosen to be 2° and this allowed a range

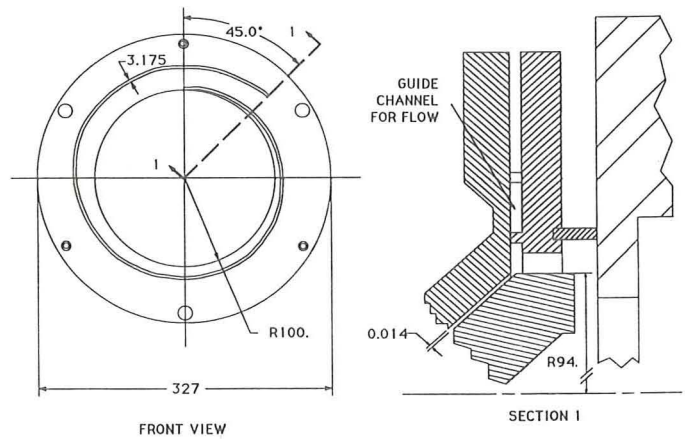

Figure 4 Installation of the inlet swirl vane in the leakage flow test apparatus.

of swirl ratios, defined as the ratio of the inlet tangential velocity to the rotor velocity. Thus, as the leakage flow rate and therefore tangential velocity was increased, the swirl ratio could be increased for a fixed rotor speed. Various views of the device are shown in figure 4.

Assuming conservation of circulation and using a continuity relation, the swirl ratio, Γ, of the inlet swirl velocity, u_θ, to the rotor speed, ωR_2, which resulted from the installed vane, was estimated to be given by

$$\Gamma = \frac{u_\theta}{\omega R_2} = \frac{Q}{B}\frac{1}{2\pi R_2^2 \omega}\frac{1}{\tan \alpha} \qquad (5)$$

The above relation implies that the flow discharging from the inlet swirl vane is parallel with that vane. However, we need to note that this was not confirmed by measurement of the inlet swirl velocity. It is also important to observe that the inlet swirl could not be varied arbitrarily as it depends on the leakage flow rate. Recalling that the flow coefficient, ϕ, is given by

$$\phi = Q/2\pi R_2^2 H\omega \qquad (6)$$

it follows that,

$$\frac{\Gamma}{\phi} = \frac{H}{B \tan \alpha} \qquad (7)$$

Therefore the only way to to vary the inlet swirl independently of the flow coefficient would be to vary the geometry of the inlet swirl vane.

4. EXPERIMENTAL RESULTS FOR ROTORDYNAMIC FORCES

Typical experimental measurements of the dimensionless normal and tangential forces, Fn and Ft, will be presented in this section. The fluid medium in which the experiments were conducted was water. The rotordynamic results from the force balance measurements were obtained for different rotating speeds of 500, 1000, 2000 RPM, different leakage flow rates (zero to 50 GPM), three different clearances, H, and two eccentricities, ε. The range of rotational Reynolds numbers was $462x10^3$-$1851x10^3$ and the range of axial flow Reynolds numbers was 2136-8546. While the rotational Reynolds numbers for the experimental flows are clearly in the developed turbulent regime, it is possible that the axial flow Reynolds numbers were too slow for the kind of resonances predicited by Childs to be manifest. Data has already been presented for experiments performed without the inlet swirl vane so that the inlet swirl ratios are close to zero. They will be summarized here, but the reader is referred to Guinzburg et al. (1992) for greater detail. The effect of inlet swirl is the primary subject of this paper.

The components of the generalized hydrodynamic force matrix that result when the impeller whirls in an eccentric orbit of 0.118 cm , at 1000 RPM, and a clearance of 0.140 cm are shown in Figure 5. Note that the general form and magnitude of the data is very similar to that obtained for impellers by Jery (1986) and Adkins (1986) and to that from Childs' model in the absence of the "resonance." One of the most significant features of these results is the range of positive whirl ratios within which the tangential force is positive and therefore potentially destabilizing rotordynamically.

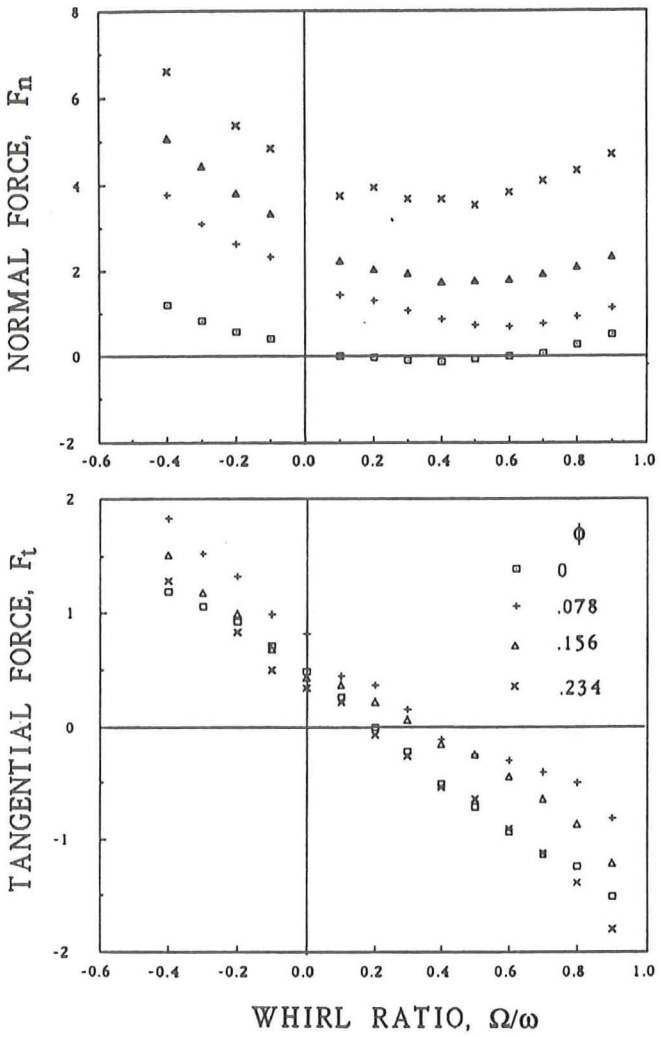

Figure 5 Dimensionless normal and tangential forces for zero inlet swirl at 1000 RPM, for an eccentricity ε=0.118 cm, a clearance H = 0.140 cm, offset δ = 0 and various flow rates as follows: 0 ℓ/sec, 0.631 ℓ/sec, 1.262 ℓ/sec, 1.892 ℓ/sec.

From other experiments, the data was determined to lie within the linear regime of small eccentricities (note that the assumption of linearity was implicit in equation l). The Bernoulli effect on the normal force increases with increasing flow at both positive and negative whirl ratios. It would also appear that the positive tangential forces at small positive whirl ratios are smallest at the highest flow rate and therefore increasing the flow is marginally stabilizing. It seems that all the forces are roughly inversely proportional to the clearance, H. For the same eccentricity and two different clearances, the smaller clearance generates larger perturbations in the flow which accentuate the acceleration in the fluid and increase the pressure differences.

Figure 6 shows data taken for a wide range of swirl conditions. This set could be compared with the data obtained for figure 5, noting that increasing the flow coefficient in figure 6 also increases the swirl ratio. Figure 7 compares data without swirl at a flow coefficient of ϕ = 0.078 to data with swirl (Γ=1.0). It can be seen that the effect of swirl is to increase the tangential force thereby

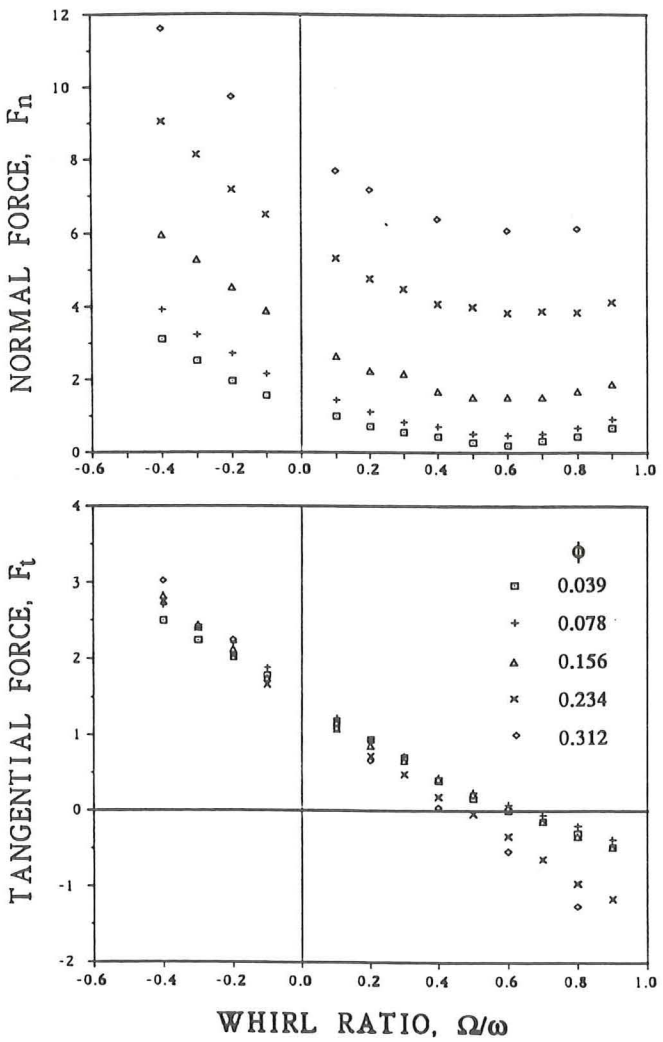

Figure 6 Dimensionless normal and tangential forces with swirl at 1000 rpm, an eccentricity ε = 0.118 cm, a clearance H = 0.140 cm, offset δ = 0 and various flow rates as follows: 0.315 ℓ/sec (Γ=0.5), 0.631 ℓ/sec (Γ=1.0), 1.262 ℓ/sec (Γ=2.0), 1.892ℓ/sec (Γ=3.0). The inlet swirl changes as the flow coefficient changes.

also increasing the range of whirl ratios for which there is a potentially destabilizing force. As the flow coefficient increases, the tangential force decreases. However, it should be noted that the flow coefficient is coupled to the swirl; therefore the swirl also increases. For the normal force, a decrease occurs with swirl for high positive whirl ratios. So the effects of flow and swirl seem to act in competition. Clearly it would be interesting to examine the case where flow is increasing and the swirl is fixed, which would require construction of additional inlet guides.

5. ROTORDYNAMIC COEFFICIENTS

Conventionally, rotordynamicists represent the force matrix by sub-dividing into components which depend on the orbit position (x,y), the orbit velocity $(\dot{x},\dot{y})$ and the orbit acceleration $(\ddot{x},\ddot{y})$. It is convenient for analytical

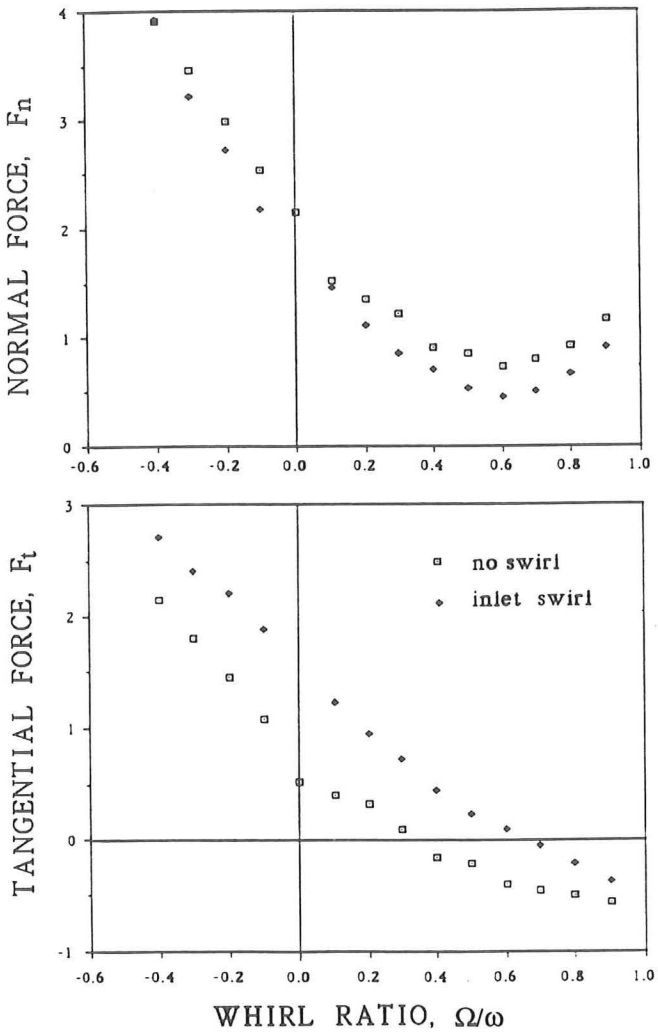

Figure 7 Comparison of the dimensionless normal and tangential forces with and without inlet swirl at 1000 rpm, an eccentricity ε = 0.118 cm, a clearance H = 0.140 cm, offset δ = 0 and a flow rate of 0.631 ℓ/sec. The inlet swirl is Γ=1.0

purposes to evaluate these components by fitting quadratics to the experimental data. Though the functional dependence of F_n on the whirl ratio is not necessarily quadratic nor is F_t linear, it is nevertheless of value to the rotordynamicists to fit the data of the figures from the previous section to the following expressions:

$$F_n = M\left(\frac{\Omega}{\omega}\right)^2 - c\left(\frac{\Omega}{\omega}\right) - K$$

$$F_t = +m\left(\frac{\Omega}{\omega}\right)^2 - C\left(\frac{\Omega}{\omega}\right) + k \qquad (8)$$

where M,C,c,K,k are the dimensionless direct added mass (M), direct damping (C), cross-coupled damping (c), direct stiffness (K) and cross-coupled stiffness (k). The cross-coupled added mass (m) will be omitted for simplicity, since a linear fit for Ft is adequate. From a stability point of view, the tangential force is most interesting; a positive cross-coupled stiffness is destabilizing because it drives the forward orbital motion of the rotor. Positive direct damping and negative cross-coupled stiffness are stabilizing because they oppose orbital motion.

Various effects such as speed, eccentricity, shroud clearance, and seal clearance have already been discussed in a separate paper (Guinzburg et al 1992). To summarize, a large negative stiffness results in a positive normal force which would tend to increase the radius of the orbital motion; increasing the leakage flow increases this force. On the other hand, a positive cross-coupled stiffness is destabilizing because it drives the forward orbital motion of the rotor so as to encourage whirl. Increased leakage flow is stabilizing in that the tangential force decreases with leakage flow. Direct damping decreases slightly with flow and would therefore be less stabilizing since the tangential force increases. Below a flow coefficient of 0.7, direct damping is negative so it would seem to encourage whirl. At higher flow rates, direct damping begins to increase, which would decrease the tangential force. However, these flow rates are not particularly meaningful as far as leakage flow rates in real pumps are concerned. The cross-coupled damping decreases slightly and the added mass term increases with flow, thus contributing to a larger normal force. In other words, inertial motion would discourage orbital motion of the impeller but drive the impeller in the direction of displacement. It is interesting to note that at higher flow rates, the trend of the added mass also changes.

The results were obtained for a range of shaft speeds from 500 RPM to 2000 RPM and shown to be independent of speed. Also, the effect of eccentricity has little effect on the normalized rotordynamic coefficients. The effect of the clearance between the rotating shroud and the stationary casing on the rotordynamic coefficients for three clearances was also explored and the normalized coefficients were shown to be roughly inversely proportional. Rotordynamically speaking, a smaller force is generated with a larger clearance. The effect of increasing the seal clearance indicated that wear of the seal is rotordynamically destabilizing.

6. INLET SWIRL EFFECTS

The effects of inlet swirl velocity are presented in figure 8. Neither the direct stiffness nor the direct damping change substantially with the addition of swirl. However, the cross-coupled damping and hence the magnitude of the normal force increase with the addition of swirl. The cross-coupled stiffness and therefore the tangential force also increase. Thus reducing the swirl to the flow would be stabilizing.

The data obtained in the present study show that the effect of inlet swirl is to increase the tangential force thereby also increasing the range of whirl ratios for which there is a potentially destabilizing force. However, inlet swirl seems to decrease the normal force at high positive whirl ratios. The effects of swirl are in contrast to the effects of increasing the leakage flow, which cause a decrease in the normal force and an increase in the tangential force. Clearly it would be interesting to examine the case where flow is increasing and the swirl is fixed. This would require construction of additional inlet swirl vanes.

The test results of Childs et al. (1990a,b) also demonstrated the favorable influence that a swirl brake has in reducing the seal destabilizing forces. Benckert and Wachter(1980) originally showed that a swirl brake, which reduces the inlet tangential velocity, would also reduce the cross-coupled stiffness. In earlier experiments on smooth seals by Childs et al.(1988), the direct damping was shown to be relatively insensitive to changes in inlet swirl, while the cross-coupled stiffness was shown to increase with swirl. The only result which is different is for the direct stiffness of smooth seals, which shows a slight increase with swirl.

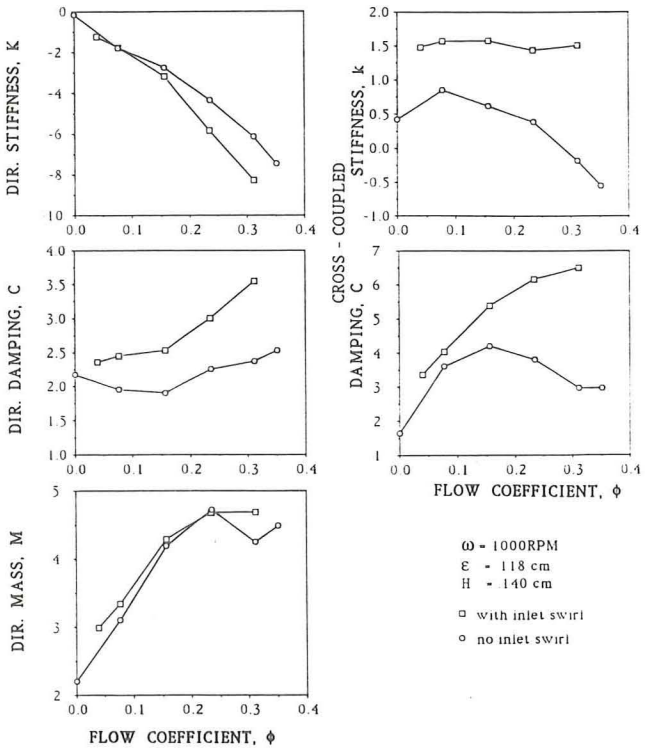

Figure 8 Rotordynamic coefficients showing the effect of inlet swirl as a function of flow coefficient for 1000 RPM and an eccentricity of 0.118 cm.

7. ROTORDYNAMIC STABILITY

The cross-coupled coefficient, k and the direct damping coefficient, C are important considerations with regard to rotordynamic stability; k and C oppose each other in trying to destabilize/stabilize the rotor. A convenient measure of the stability is the ratio of cross-coupled stiffness to direct damping k/C, which would estimate the whirl ratio at which the force would no longer be destabilizing. For circular synchronous orbits, it provides a ratio between the destabilizing force due to k and the stabilizing force due C. Thus, reducing the ratio of k/C improves the stability of the rotor system.

Figure 9 shows the effect of swirl on the whirl ratio. The tangential velocity of the bulk flow will clearly decrease as the flow increases. It can be seen that as the flow increases, the whirl ratio decreases. This trend agrees with Childs et al.(1988) wherein the whirl frequency ratio decreases as the swirl decreases. While the present experiment involves a different geometry from the bearing model, the whirl frequency ratio, k/C is of the same order of magnitude as the heuristic proposal which Crandall (1982) applied to the Sommerfeld bearing model.

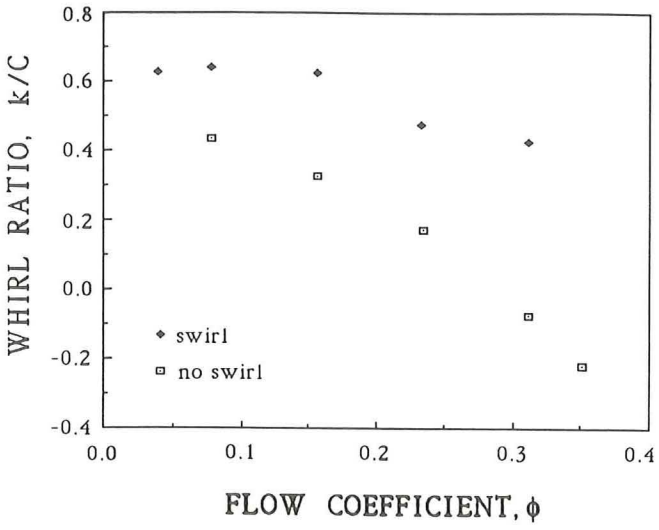

Figure 9 Whirl ratio with and without the inlet swirl vane for an eccentricity, ε=0.118 cm, a speed of 1000 RPM, a clearance, H=0.140 cm and an offset, δ = 0 as a function of flow coefficient.

8. CONCLUSIONS

A review of the existing experimental and analytical results shows that the discharge-to-suction leakage flow in a centrifugal pump can contribute substantially to the fluid-induced rotordynamic forces for that turbomachine. This motivated the current experimental study of leakage flows between the shroud and the stationary casing of a centrifugal pump and their rotordynamic effects. The focus was to investigate the dependency of the normal and tangential forces on the swirl at the inlet to the leakage path. Experimental results for simulated leakage flows of rather simple geometry have been presented for different whirl frequencies and flow rates. As with previous results for impellers, the forces scaled with the square of the rotor speed. The functional dependence on whirl frequency to rotating frequency ratio (termed the whirl ratio) is very similar to that measured in experiments and to that predicted in the theoretical work of Childs.

The effect of swirl is to increase the tangential force thereby also increasing the range of whirl ratios for which there is a potentially destabilizing force. Thus reducing the swirl to the flow would be stabilizing. As for the normal force, swirl seems to decrease the force at higher positive whirl ratios. The effects of swirl are in contrast to the effects of increasing the leakage flow, which cause a decrease in the normal force and an increase in the tangential force. Clearly it would be interesting to examine the case where flow is increased while the swirl remains fixed. This would, however, require the construction of additional inlet guides. Finally, experiments which included the addition of a wide range of prescribed inlet swirl ratios showed none of the "resonances" predicted by Childs.

ACKNOWLEDGEMENTS

The assistance provided by F. Zhuang, A. Bhattacharyya, F. Rahman and Sandor Nagy with the experimental program is greatly appreciated. We would also like to thank NASA George Marshall Space Flight Center for support under Grant NAG8-118.

REFERENCES

Adkins, D.E. 1986. Analyses of hydrodynamic forces on centrifugal pump impellers. Ph.D. Thesis, California Institute of Technology, Pasadena, Calif.

Adkins, D.R., and Brennen, C.E. 1988. Analyses of Hydrodynamic Radial Forces on Centrifugal Pump Impellers. ASME J. Fluids Eng., Vol. 110, No. 1, pp. 20-28.

Benckert, H. and Wachter, J. 1980. Flow Induced Spring Coefficients of Labyrinth Seals for Application in Rotor Dynamics. Workshop on Rotordynamic Instability Problems in High Performance Turbomachinery, pp. 189-212.

Bolleter, U., Wyss, A., Welte, I., Stürchler, R. 1987. Measurement of Hydrodynamic Interaction Matrices of Boiler Feed Pump Impellers. ASME J. Vibration, Acoustics, Stress, and Reliability in Design, Vol. 109, pp. 144-151.

Bolleter, U., Leibundgut, E., Sturchler, R. 1989. Hydraulic Interaction and Excitation Forces of High Head Pump Impeller. Pumping Machinery- 1989, Vol. 81, 3rd Joint ASCE/ASME Mechanics Conference, UCSD, July 9-12, 1989, pp. 187-193.

Chamieh, D.S. 1983. Forces on a Whirling Centrifugal Pump-Impeller. Ph.D. Thesis, Division of Engineering and Applied Science, California Institute of Technology, Pasadena, CA.

Chamieh, D.S., Acosta, A.J., Brennen, C.E., Caughey, T.K. 1985. Experimental Measurements of Hydrodynamic Radial Forces and Stiffness Matrices for a Centrifugal Pump-Impeller. ASME Journal of Fluids Engineering, Vol. 107, No.3, pp. 307-315.

Childs, D.W. 1986. Force and Moment Rotordynamic Coefficients for Pump-Impeller Shroud Surfaces. Proceedings of Advanced Earth-to-Orbit Propulsion Technology Conference, Hunstville, AL, May 1986, NASA Conf Publ. 2436, pp. 296-326.

Childs, D.W., Elrod, D., Hale, K. 1988. Annular Honeycomb Seals: Test Results for Leakage and Rotordynamic Coefficients; Comparisons to Labyrinth and Smoooth Configurations. 3rd Conference on Advanced Earth-to-Orbit Propulsion Technology, Huntsville, Alabama, May, 1988, pp. 79-94.

Childs, D. W. 1989. Fluid Structure Interaction Forces at Pump-Impeller-Shroud Surfaces for Rotordynamic Calculations. ASME J. Vibration, Acoustics, Stress, and Reliability in Design, Vol. 111, pp. 216-225.

Childs, D. W., Ramsey, C. 1990a. Seal-Rotordynamic-Coefficient Test Results for a Model SSME ATD-HPFTP Turbine Interstage Seal with and without Swirl Brake. Joint ASME/STLE Tribology Conference, Toronto, Canada, October 7-10, Paper No. 90-Trib-12.

Childs, D. W., Baskharone, E., Ramsey, C. 1990b. Test Results for Rotordynamic Coefficients of the SSME HPOTP Turbine Interstage Seal with Two Swirl Brakes. Joint ASME/STLE Tribology Conference, Toronto, Canada, October 7-10, Paper No. 90-Trib-45.

Crandall, Stephen H. 1982. Heuristic Explanation of Journal Bearing Instability. Rotordynamic Instability Problems of High Performance Turbomachinery. NASA Conference Publication 2250, pp. 274-283.

Domm, U. and Hergt, P. 1970. Radial forces on impeller of volute casing pumps. Flow Research on Blading, editor L.S. Dzung, Elsevier Publ. Co., Netherlands, pp. 305-321.

Franz, R., Acosta, A.J., Brennen, C.E., Caughey, T.K. 1989. The Rotordynamic Forces on a Centrifugal Pump Impeller in the Presence of Cavitation. Proceedings of 3rd Joint ASCE/ASME Mechanics Conference, UCSD, July 1989, Pumping Machinery, Vol. 81, pp. 205-212.

Guinzburg, A., Brennen, C.E., Acosta, A.J. and Caughey, T.K. 1990. Rotordynamic forces generated by discharge-to-suction leakage flows in centrifugal pumps. NASA CP-3092.

Guinzburg, A., Brennen, C.E., Acosta, A.J. and Caughey, T.K. 1990. Measurements of the rotordynamic shroud forces for centrifugal pumps. ASME Turbomachinery Forum, Toronto, Canada, June 1990.

Guinzburg, A. 1992. Rotordynamic forces generated by discharge-to-suction leakage flows in centrifugal pumps. Ph.D. Thesis, Division of Engineering and Applied Science, California Institute of Technology, Pasadena, CA.

Guinzburg, A., Brennen, C.E., Acosta, A.J. and Caughey, T.K. 1992. The rotordynamic characteristics of leakage flows in centrifugal pumps. To be presented at the 1992 NFDC.

Hawkins, L. and Childs D.W. 1988. Experimental Results for Labyrinth Gas Seals with Honeycomb stators: Comparisons to Smooth-Stator Seals and Theoretical Predictions. 3rd Conference on Advanced Earth-to-Orbit Propulsion Technology, Huntsville, Alabama, May, 1988, pp. 94-111.

Hergt, P. and Krieger, P. 1969-70. Radial forces in centrifugal pumps with guide vanes. Proc. Inst. Mech. Eng., Vol. 184, Part 3N, pp. 101-107.

Iversen, H.W., Rolling, R.E., and Carlson, J.J. 1960. Volute Pressure Distribution, Radial Force on the Impeller and Volute Mixing Losses of a Radial Flow Centrifugal Pump. ASME Journal of Eng.ineering for Power, Vol. 82, No. 2, pp. 136-144.

Jery, B. 1986. Experimental Study of Unsteady Hydrodynamic Force Matrices on Whirling Centrifugal Pump Impellers. Ph.D Thesis, California Institute of Technology.

Jery, B., Acosta, A.J., Brennen, C.E., and Caughey, T.K. 1985. Forces on Centrifugal Pump Impellers. Second International Pump Symposium, Houston, Texas, April 29-May 2, 1985.

Zhuang, F. 1989. Experimental Investigation of the Hydrodynamic Forces on the Shroud of a Centrifugal Pump Impeller. E249.9, Division of Engineering and Applied Science, California Institute of Technology.